https://doi.org/10.5194/essd-2022-178
Preprint. Discussion started: 23 June 2022

Open Access Earth System Science Data Discussions

SDUST2020 MSS: A global 1′×1′ mean sea surface model determined from multi-satellite altimetry data

Jiajia Yuan[1,2], Jinyun Guo[1], Chengcheng Zhu[1,3], Zhen Li[1], Xin Liu[1], Jinyao Gao[4]

[1]College of Geodesy and Geomatics, Shandong University of Science and Technology, Qingdao, Shandong, China
[2]School of Geomatics, Anhui University of Science and Technology, Huainan, Anhui, China
[3]School of Surveying and Geo-Informatics, Shandong Jianzhu University, Jinan, Shandong, China
[4]Second Institute of Oceanography of MNR, Hangzhou, Zhejiang, China

Correspondence to: Jinyun Guo (jinyunguo1@126.com)

Abstract. This article focuses on the determination and the validation of a new global mean sea surface (MSS) model which is named as SDUST2020 (Shandong University of Science and Technology 2020) with a grid of 1′×1′. This new model is established with 19-year moving average method and merges multi-satellite altimetry data over 27-year (from January 1993 to December 2019). The data of HY-2A, Jason-3 and Sentinel-3A are first ingested in the SDUST2020 MSS, but not in any other global MSS model, such as CLS15 and DTU18 MSS models. Validations, including the comparison with CLS15 and DTU18 MSS models, the comparison with GPS-leveled tide gauges and the comparison with altimeter data, are performed to estimate the quality of the SDUST2020 MSS model, and all the results show that the SDUST2020 MSS model is accurate and reliable. The SDUST2020 MSS dataset are freely available at the site (data DOI: https://doi.org/10.5281/zenodo.6555990, Yuan et al., 2022).

1 Introduction

Mean sea surface (MSS) is a relative steady-state sea level within a finite time span, which has the important applications in geodesy, oceanography and other disciplines (Andersen and Knudsen, 2009; Schaeffer et al., 2012; Andersen et al., 2018; Pujol et al., 2018; Guo et al., 2022). It is obtained by time averaging the instantaneous sea surface height (SSH) observed by altimeter over a finite time span (Andersen and Knudsen, 2009). However, sea level contains a variety of variation information about time scale. To completely separate the mean and time-varying part of sea level, it is necessary to continuously collect SSH data in time and space. It is a challenge for establishing an MSS model to accurately filter time-varying sea level signals and obtain high-resolution mean SSH data within a finite time span.

Since the 1970s, studies of MSS model have never been interrupted after the success of Geos-3 satellite altimetry data. Every update of satellite altimetry data is accompanied by the establishment of some new MSS models. Moreover, the precision and grid size of the MSS model are gradually improving and enhancing with the development of the satellite altimetry

https://doi.org/10.5194/essd-2022-178
Preprint. Discussion started: 23 June 2022


Open Access Earth System Science Data Discussions

technique. So, it can be said that the development of MSS model is an epitome of the development history of satellite altimetry technology.

At present, only two research institutions, the Centre National d'Etudes Spatiales (CNES) and the space research center of the Technical University of Denmark (DTU), are constantly updating and publishing new MSS models. For example, the series MSS models CNES_CLS11 (Schaeffer et al., 2012), CNES_CLS15 (Pujol et al., 2018) and CNES_CLS19 (ongoing to compute) are published by CNES, and the series MSS models DTU10 (Andersen et al., 2010), DTU13 (Andersen et al., 2015), DTU15 (Andersen et al., 2016) and DTU18 (Andersen et al., 2018) are published by DTU. Among them, CNES_CLS15 (abbreviation for CLS15) and DTU18 are the latest MSS models and have the same fundament which is the mean profile of Topex/Poseidon (T/P), Jason-1 and Jason-2 span from 1993 to 2012. They all have a grid size of 1′×1′, but the spatial coverage and altimetry data used are different. For example, the global coverage of CLS15 model is 80°S~84°N, while that of DTU18 model is 90°S~90°N. CLS15 model ingest the exact repeat missions (ERM) data (T/P, Jason-1, Jason-2, ERS-2, Envisat, GFO), as well as the geodetic missions (GM) data (ERS-1/GM, Jason-1/GM, Cryosat-2). Compared with CLS15, DTU18 replaces GFO data with SARAL/ERM data and ERS-1/GM data with SARAL Drifting Phase (DP) data.

With the continuous development of satellite altimetry technology, the types and quantity of available SSH data are also increasing: on the one hand, it comes from altimetry satellites in orbit; on the other hand, it comes from the newly launched altimetry satellites. Multi-satellite altimetry data will be fused to establish an MSS model over a longer time span. Among these altimeter data, HY-2A, Jason-3, and Sentinel-3A have not been ingested in any global MSS models (e.g. CLS15, DTU18). These altimeter data will be used together with other altimeter data (e.g. T/P, Jason-1, Jason-2, ERS-1, ERS-2, Envisat, GFO, Cryosat-2 and SARAL) to establish the new global MSS model, called SDUST2020 (Shandong University of Science and Technology 2020) model.

Ocean tide is one of the main sources of errors that affect altimetry data's quality. After tidal error correction, there is still a certain residual error, which cannot be ignored to an MSS model (Yuan et al., 2020). Therefore, a new method, the 19-year (corresponding to the 18.61-year cycle signal of ocean tide) moving average method, will be used to establish the SDUST2020 model with a grid size of 1′×1′ from multi-satellite altimetry data span from 1993 to 2019. This new method has been proved to be effective in improving the accuracy of the established MSS model in Yuan et al (2020).

2 Data sources

2.1 Satellite altimetry data

Multi-satellite altimetry data used in this paper are selected from the along-track Level-2p (L2P; version_02_00) products which released by Archiving Validation and Interpretation of Satellite Oceanographic Data (AVISO) (CENS, 2017). The

https://doi.org/10.5194/essd-2022-178
Preprint. Discussion started: 23 June 2022


Open Access Earth System Science Data Discussions

L2P products contains multi-satellite altimetry data, including ERS-1, T/P, ERS-2, GFO, Jason-1, Envisat, Jason-2, Cryosat-2, HY-2A, SARAL, Jason-3, Sentinel-3A and Sentinel-3B. They are generated by the 1 Hz mono mission along-track altimetry data through various error corrections, data editing and quality control, unification of reference ellipsoid (adjusted to have the same reference ellipsoid as T/P), and other data processing (CENS, 2017). The error corrections for each mission are detailed in the along-track L2P products handbook (CENS, 2017), which include instrumental errors, environmental perturbations (wet tropospheric, dry tropospheric and ionospheric effects), the ocean sea state bias, the tide effect (ocean tide, solid earth tide and pole tide) and atmospheric pressure (combining atmospheric correction: high frequency fluctuations of the sea surface topography and inverted barometer height correction).

Multi-satellite altimetry data span from 1 January 1993 to 31 December 2019 selected from L2P products are shown in Table 1. Full-year ERM data are selected to make altimeter data less contaminated by the oceanic seasonal variability and the interannual signal after collinear adjustment (Schaeffer et al., 2012; Pujol et al., 2018). The data of the ERS-1/GM, Cryosat-2, Jason-1/GM, HY-2A/GM and SRL/DP are used to improve the spatial resolution of the MSS model. All the data of the ERM and GM data are jointly used to establish the SDUST2020 model.

Table 1. Multi-satellite altimetry data used in this study.

Missions	Time span	Cycles	Missions	Time span	Cycles
T/P	1993.01.01–2002.08.11	011–364	SARAL	2013.03.14–2015.03.19	001–021
Jason-1	2002.08.11–2009.01.26	022–259	HY-2A	2014.04.12–2016.03.15	067–117
Jason-2	2009.01.26–2016.10.02	021–303	Sentinel-3A	2016.06.28–2018.12.31	006–039
Jason-3	2016.10.02–2019.12.31	024–143	ERS-1/GM	1994.04.10–1995.03.21	030–040
ERS-2	1995.05.15–2003.06.02	001–084	Cryosat-2	2011.01.28–2019.12.12	014–125
GFO	2001.01.07–2008.01.18	037–208	Jason-1/GM	2012.05.07–2013.06.21	500–537
Envisat	2002.09.30–2010.10.18	010–093	HY-2A/GM	2016.03.30–2019.12.30	118–270
T/P Tandem	2002.09.20–2005.09.24	369–479	SARAL /DP	2016.07.04–2019.12.16	100–135
Jason-1 Tandem	2009.02.10–2012.02.15	262–372			

2.2 The data of GPS-leveled tide gauges around Japan

The data of tide gauges are downloaded from the Permanent Service for Mean Sea Level (PSMSL) website (www.psmsl.org/). PSMSL is responsible for the collection, publication, analysis and interpretation of sea level data from the global network of tide gauges (Holgate et al., 2013). It provides the monthly and annual mean values for each tide gauges, and these mean values have been reduced to a common datum called Revised Local Reference (RLR) datum. This reduction is performed by the PSMSL making use of the tide gauge datum history provided by the supplying authority. In order to avoid negative numbers in the resulting RLR monthly and annual mean values, an offset of 7000 mm is also made.

https://doi.org/10.5194/essd-2022-178
Preprint. Discussion started: 23 June 2022

The data of GPS stations are obtained from the Système d'Observation duNiveau des Eaux Littorales (SONEL) website (www.sonel.org). The SONEL provides the URL6b GPS daily data calculated by the University of La Rochelle (ULR) with GAMIT/GLOBK software, and the GPS data have been corrected for emergencies such as earthquakes (Santamaria-Gomez et al., 2017).

The sea level observed from satellite altimeter is relative to the reference ellipsoid. However, the sea level obtained from the tide gauges is relative to a certain benchmark (e.g. RLR). Therefore, there are differences between these two surfaces. Fortunately, the ellipsoidal height of RLR can be obtained by GPS (equipped on the tide gauges) observation, which can be used to unify the sea level obtained by the tide gauges to the reference ellipsoid. Figure 1 shows the relationship among the sea level observed from the satellite altimeter that is relative to the reference ellipsoid, the sea level obtained from the tide gauges that is relative to the RLR, and the height of RLR derived from GPS that is relative to the reference ellipsoid.

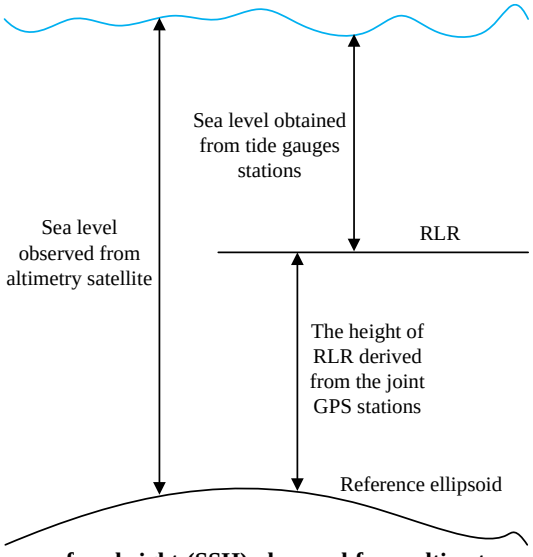

Figure 1. The relationship among the sea surface height (SSH) observed from altimetry satellite, the relative SSH obtained from tide gauges above the RLR (Revised Local Reference), and the height of RLR derived from the joint GPS stations above the reference ellipsoid.

There are about 34 tide gauges around Japan on the PSMSL website, which have continuous annual data span from 1993 to 2019 and have joint GPS data. The information of 34 tide gauges stations and joint GPS stations around Japan are shown in the Appendix of this study. The data of GPS-leveled tide gauges around Japan are selected to validate the SDUST2020 MSS model.

https://doi.org/10.5194/essd-2022-178
Preprint. Discussion started: 23 June 2022

Open Access Earth System Science Data Discussions

3 Methodology

Figure 2 shows the data processing process for establishing the SDUST2020 model. Firstly, the multi-satellite altimetry data (as shown in Table 1) span from January 1, 1993 to December 31, 2019 selected from L2P products are grouped into 19-year-long moving windows shifted by one year start from January 1993, and then nine groups of multi-satellite altimetry data will be obtained. Secondly, the multi-satellite altimetry data of each group are processed, including collinear adjustment of ERM data, ocean variability correction of GM data (addressed by objective analysis and polynomial fitting interpolation), multi-satellite joint crossover adjustment, and the least-squares collocation (LSC) technique for gridding. Thirdly, the MSS models with a grid size of 1'×1' are established respectively, so nine MSS models with the same grid size will be obtained. Finally, the SDUST2020 model is obtained by weighting the weighted average value of the nine models according to the reciprocal square of the estimated SSH error at the same grid point. The calculation method is shown in equation (1) and (2).

$$mssh_{i,\mathrm{SDUST2020}} = \frac{\sum_{j=1}^{9}\left(mssh_{i,j}/\left(err_{i,j}\right)^2\right)}{\sum_{j=1}^{9} 1/\left(err_{i,j}\right)^2} \tag{1}$$

$$err_{i,\mathrm{SDUST2020}} = \frac{1}{\sqrt{\sum_{j=1}^{9} 1/\left(err_{i,j}\right)^2}} \tag{2}$$

where $mssh_{i,\mathrm{SDUST2020}}$ and $err_{i,\mathrm{SDUST2020}}$ are the SSH and the error of the SSH at the grid point i in the SDUST2020 model, respectively; $mssh_{i,\mathrm{SDUST2020}}(j = 1,\cdots,9)$ and $err_{i,j}(j = 1,\cdots,9)$ are the SSH and the error of the SSH at the grid point i in each of the nine MSS models, respectively.

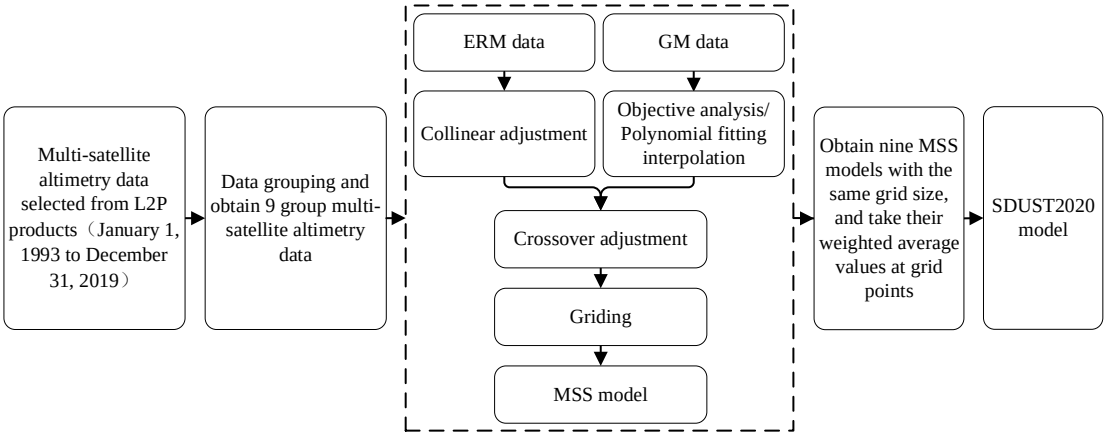

Figure 2. Data processing process of L2P products to establish the SDSUT2020 model.

3.1 Ocean variability correction

Ocean variability correction of altimeter data is a major difficulty in the process of establishing an MSS model (Schaeffer et al., 2012; Pujol et al., 2018). Since the ground tracks of altimetry satellite with ERM are coinciding with each other, so the ocean variability correction of ERM data can be solved by the method of collinear adjustment. This method makes it

https://doi.org/10.5194/essd-2022-178
Preprint. Discussion started: 23 June 2022

possible to remove the ocean variability (seasonal and interannual), but also to obtain the mean along-track SSH. The method of collinear adjustment used in this study is the same as that described in yuan et al. (2021).

Since the GM data does not have the characteristics of repeated periods like ERM data, so the ocean variability correction of GM data cannot be addressed by the method of collinear adjustment. Fortunately, the ocean variability of GM data has been simultaneously obtained by ERM data. For example, ERS-1/GM data contains the same ocean variability as T/P data in the same period 1994-1995. Currently, the main methods for the correction of GM data for ocean variability are the objective analysis or based on the use of polynomial functions (e.g. polynomial fitting interpolation, PFI). The objective analysis method is considered as the best method to correct the ocean variability of GM data (Schaeffer et al., 2012; Pujol et al., 2018), and has been applied successfully to the establishing of MSS models, such as models CLS11 and CLS15. It can be used to interpolate the ocean variability of one or more missions considered as a reference at the spatial and temporal position of the satellite that would be corrected for ocean variability (Schaeffer et al., 2012). The objective analysis method used in this study is described in yuan et al. (2021) and further details are also given in Le Traon et al. (1998; 2001; 2003) and Ducet et al. (2000).

As we all know, the T/P series (refer to T/P, Jason-1, Jason-2 and Jason-3) satellite altimetry data have the highest measuring accuracy. Therefore, the mean along-track SSH of continuous T/P series during 1993-2019 are used as the fundament to calculate the ocean variability of ERM data. Since the orbit inclination of T/P series satellites are about 66°, while that of satellite with GM are usually greater than 66°. For example, the orbit inclination of ERS-1/168, HY-2A/GM, SARAL/DP and Cryosat-2 are 98.52°, 99.3°, 98.55° and 92°, respectively. So, the objective analysis method can only correct the ocean variability of GM data within the latitude range of 66°S to 66°N, while that of beyond 66°S or 66°N cannot be corrected. In this study, when correcting GM data (such as ERS-1/168, HY-2A/GM, SARAL/DP and Cryosat-2) for ocean variability, the objective analysis method is adopted for the GM data between 66°S and 66°N, while the PFI method is adopted for GM data beyond 66°S or 66°N.

The basic principle of method PFI can be expressed as: firstly, a fitting polynomial is used to fit the grid sea level variation time series to extract the ocean variability, and the least squares solution is carried out to solve the fitting parameters; secondly, the ocean variability of GM data (above 66°S or 66°N) are interpolated with time as the independent variable, so as to realize the ocean variability correction of GM data. The grid sea level variation time series are monthly averaged grid sea level variation time series between 1993 and 2019 provided by AVISO, with a grid of 15′×15′. The fitting polynomial is (Andersen et al., 2006; Andersen and Knudsen, 2009; Jin et al., 2016):

$$y = k + b \cdot t + c \cdot \cos(2 \cdot \pi \cdot t) + d \cdot \sin(2 \cdot \pi \cdot t) + e \cdot \cos(4 \cdot \pi \cdot t) + f \cdot \sin(4 \cdot \pi \cdot t) \quad (3)$$

where y is the sea level variation time series; t is the time; k is the bias; b is the trend; c and d are the coefficients of the annual signal; e and f are the coefficients of the semi-annual signal.

https://doi.org/10.5194/essd-2022-178
Preprint. Discussion started: 23 June 2022


Open Access Earth System Science Data Discussions

3.2 Crossover adjustment

The crossover adjustment is an important method for the data fusion of multi-satellite altimetry (Huang et al., 2008). The method of crossover adjustment is carried out in two steps: (1) condition adjustment method, and, (2) filtering and predicting of the observational corrections along each track. In the process of crossover adjustment, an error model is established to reflect the combined effect of the various sources of error on the altimeter data. These errors are the radial orbit error, residual ocean variation, residual geophysical corrections, and so on. The error model can be expressed as (Huang et al., 2008; Yuan et al., 2020; 2021):

$$f(t) = a_0 + a_1 \cdot (t - T_0) + \sum_{j=1}^{n} \left(b_i \cdot \cos\left(j \cdot \omega \cdot (t - T_0)\right) + c_i \cdot \sin\left(j \cdot \omega \cdot (t - T_0)\right) \right) \quad (4)$$

where t is the observation time; a_0, a_1, b_i, and $c_i (i = 1, \cdots, n)$ are model parameters to be solved; ω represents the angular frequency corresponding to the duration of a surveying track ($\omega = 2\pi/(T_1 - T_0)$, where T_0 and T_1 represent the start and end times of the surveying track, respectively); and n is a positive integer determined by the length of the track. Based on empirical evidence, n is proposed to be 1–2 for a short track, 3–5 for a middle-long track, and 6–8 for a long track (Huang et al., 2008; Yuan et al., 2020).

Since the mean along-track SSH of continuous T/P series derived from the collinear adjustment is used as the fundament of the MSS model, it will remain unchanged and just correct crossover differences for other satellite altimetry data in the process of multi-satellite joint crossover adjustment. The details about the method of crossover adjustment used in this study are given in Yuan et al. (2020; 2021).

3.3 Gridding

In this study, the LSC technique (Hwang, 1989; Rapp and Bašić, 1992) is used for gridding. It has been proven to be the most suitable method for gridding (Jin et al., 2016). In the process of gridding with the LSC, a second-order Markov process is used to describe the two-dimensional isotropic covariance function to obtain the prior statistical information about the altimeter data and improve the accuracy of gridding. The process can be expressed as (Jordan, 1972; Moritz, 1978):

$$\mathrm{D}(d) = D_0 \cdot (1 + d/\alpha) \cdot e^{-d/\alpha} \quad (5)$$

where d is the two-dimensional distance between the observation point and the grid point; D_0 is the local variance parameter, which can be expressed as the variance of all observed data participating in gridding within the local range; and α is the correlation length (where a 50% correlation is obtained). Moreover, accuracy of $1/\sqrt{2}$ times of the single-satellite's crossover differences after the crossover adjustment is introduced into the LSC as the noise of the corresponding satellite data.

In the process of gridding, it should be ensured that the number of observation points within the range determined by the given search radius should be no less than 20, and the search radius is usually twice the grid spacing (e.g. 1′). When the

https://doi.org/10.5194/essd-2022-178
Preprint. Discussion started: 23 June 2022

number of observation points within the given search radius is less than 20, the search radius should be appropriately expanded until the conditions are met. The search method is to ensure five observation data points at least in each quadrant within the specified search range in the four quadrants centered on the grid point. The purpose of this method is to ensure that the observation data points around the grid point are uniformly distributed, which is conducive to ensuring the accuracy of grid data.

To improve the computational efficiency of gridding with the LSC, the globe is divided into several blocks, namely, 20°×20° blocks in the range of 80°S-60°N and 0°-360°, and 126 blocks in total. In the range of 60°N-80°N and 0°-360°, 24°×20° blocks are divided into 18 blocks. In this way, the globe is divided into a total of 144 blocks, of which there are only 141 blocks have SSH observations, while two blocks (40°N-60°N, 60°W-100°W) in the Asian continent, and one block (40°N-60°N, 240°W-260°W) in the American continent have no SSH observations. After gridding these 141 blocks, the number of 141 grids SSH data are merged. When merging, the SSH of grid points on the repeated latitude lines and longitude lines is the SSH weighted average of grid points in the adjacent two blocks, and the weight is determined by the reciprocal of the square of the SSH error estimate at the grid points, to obtain the final gridded global MSS model.

4 Results and discussion

4.1 Processing results and analysis of altimetry data

Ocean variability correction can eliminate or weaken the influence of sea level long-wave ocean variation signals, partial satellite radial orbit errors and residual errors after correction of geophysical and environmental errors. Ocean variability correction is conducted for the altimeter missions in Table 1 in global ocean, and the SSHs of these missions before and after ocean variability correction are compared with SDUST2020 model, respectively. The statistical results of the comparisons are shown in Table 2, which shows that the impact of removing the ocean variability. It can be seen from Table 2 that the variance of the difference (between the SSH of each satellite altimetry missions and the SDUST2020 model) decrease from decimeter magnitude to centimeter magnitude RMS. Among them, the RMS of T/P series (T/P+Jason-1+Jason-2+Jason-3) after ocean variation correction is the smallest, which is 0.0119 m.

Table 2. Statistical results of comparisons between heights of different altimeter missions and SDUST2020 model before and after oceanic variability correction (Unit: m).

Missions	Before ocean variation correction			After ocean variation correction		
	Mean	STD	RMS	Mean	STD	RMS
T/P+Jason-1+Jason-2+Jason-3	0.0050	0.1038	0.1040	0.0018	0.0117	0.0119
(T/P +Jason-1) Tandem	0.0079	0.1006	0.1009	0.0029	0.0160	0.0163
ERS-2	-0.0128	0.1105	0.1112	-0.0191	0.0231	0.0300
GFO	-0.0100	0.1053	0.1057	-0.0126	0.0202	0.0238
Envisat	0.0023	0.0986	0.0986	0.0008	0.0202	0.0202
HY-2A	0.0571	0.1329	0.1446	0.0376	0.0426	0.0569
SARAL	0.0256	0.0987	0.1020	0.0220	0.0331	0.0397

https://doi.org/10.5194/essd-2022-178
Preprint. Discussion started: 23 June 2022

Sentinel-3A	0.0437	0.0996	0.1088	0.0390	0.0318	0.0504
SARAL/DP	0.0387	0.0995	0.1068	-0.0018	0.0595	0.0595
ERS-1/GM	-0.0391	0.1075	0.1144	-0.0053	0.0676	0.0678
Jason-1/GM	0.0179	0.0978	0.0994	0.0007	0.0576	0.0576
Cryosat-2	0.0268	0.1022	0.1056	-0.0023	0.0612	0.0612
HY-2A/GM	0.0363	0.1024	0.1087	-0.0035	0.0639	0.0639

Figure 3 and 4 show what can be achieved by correcting the ocean variability of Jason-1/GM. Figure 3 shows the differences between SSH of Jason-1/GM and SDUST2020 model where the ocean variability have not been corrected. Before the application of this correction, the differences of SSH are dominant in the western boundary currents. However, these differences are improved significantly after the correction of ocean variability (as shown in Figure 4).

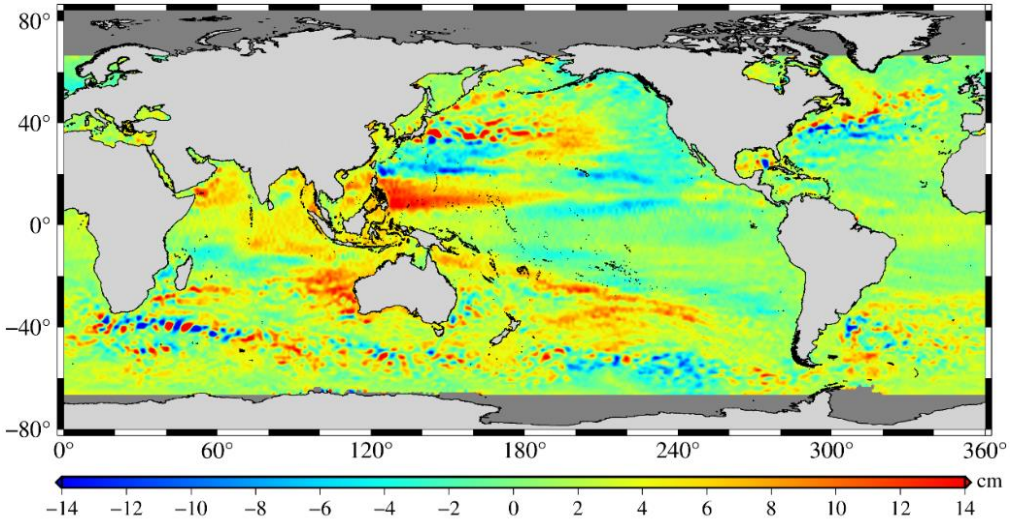

Figure 3. Sea surface heights differences between Jason-1/GM and SDUST2020 model before oceanic variability correction.

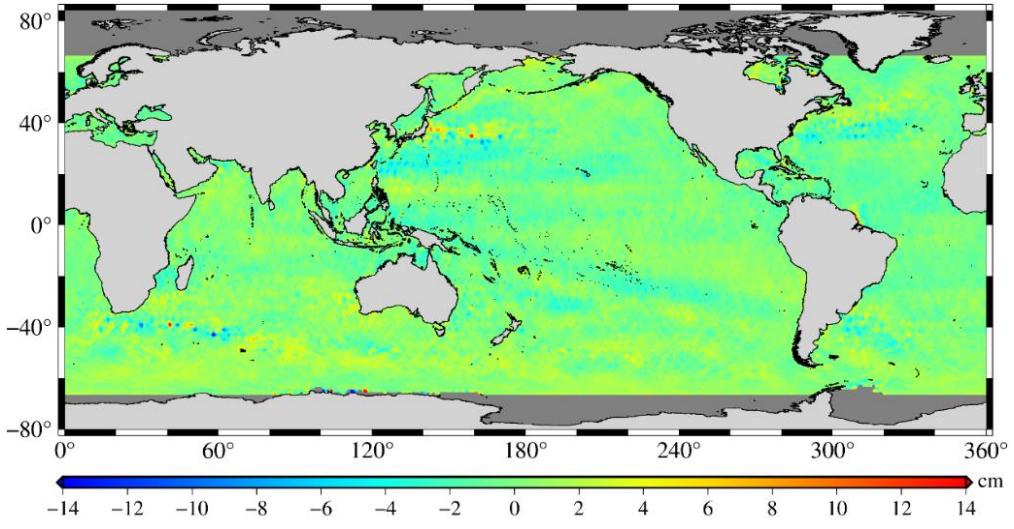

Figure 4. Sea surface heights differences between Jason-1/GM and SDUST2020 model after oceanic variability correction.

https://doi.org/10.5194/essd-2022-178
Preprint. Discussion started: 23 June 2022

All the altimeter missions in Table1 are carried out the self-crossover adjustment respectively after finishing the correction of ocean variability. Table 3 shows the statistical results of crossover differences of these missions before and after self-crossover adjustment. It can be seen from the results in Table 3 that the accuracy of all the missions has been greatly improved after self-crossover adjustment. The accuracy of ERM data is improved by about 1 cm from 1-2 cm before adjustment to about 1 cm after adjustment, and that of the GM data is improved by about 2 cm from 7-9 cm to 6-7 cm. Moreover, since the accuracy of ERM data (average accuracy of about 1 cm) is much higher than GM data (average accuracy of about 6 cm), and the accuracy of different missions are also different. Therefore, the accuracy of each missions will be considered in the process of multi-satellite joint crossover adjustment and the gridding with LSC.

Table 3. Statistical results of crossover differences of different altimeter missions before and after self-crossover adjustment (Unit: m).

Missions	Before crossover adjustment			After crossover adjustment		
	Mean	STD	RMS	Mean	STD	RMS
T/P+Jason-1+Jason-2+Jason-3	-0.0003	0.0098	0.0098	-0.0001	0.0047	0.0047
(T/P +Jason-1) Tandem	0.0001	0.0089	0.0089	0.0001	0.0060	0.0060
ERS-2	-0.0003	0.0217	0.0217	-0.0002	0.0104	0.0104
GFO	0.0003	0.0131	0.0131	0.0001	0.0077	0.0077
Envisat	0.0001	0.0208	0.0208	0.0001	0.0095	0.0095
HY-2A	0.0016	0.0238	0.0239	0.0004	0.0074	0.0075
SARAL	-0.0006	0.0219	0.0219	-0.0002	0.0134	0.0134
Sentinel-3A	-0.0001	0.0212	0.0212	-0.0001	0.0102	0.0102
SARAL/DP	0.0006	0.0835	0.0835	0.0003	0.0629	0.0629
ERS-1/GM	-0.0004	0.0899	0.0899	-0.0002	0.0708	0.0708
Jason-1/GM	-0.0015	0.0753	0.0753	-0.0008	0.0632	0.0632
Cryosat-2	0.0010	0.0824	0.0824	0.0006	0.0664	0.0664
HY-2A/GM	0.0003	0.0867	0.0867	0.0001	0.0658	0.0658

4.2 Establishment of the SDUST2020 model

According to the process of data processing in Figure 2, the SDUST 2020 model is established with 19-year moving average method from multi-satellite altimetry data (shown in Table 1). The SDSUT2020 model is shown in Figure 5. It has a grid size of 1'×1' and a global coverage range of 80°S-84°N, with a reference time span from January 1, 1993 to December 31, 2019. As can be seen from Figure 5, the global MSS is generally uneven, with the highest SSH of about 88 m and the lowest SSH of about 106 m, with a difference of 194 m.

https://doi.org/10.5194/essd-2022-178
Preprint. Discussion started: 23 June 2022

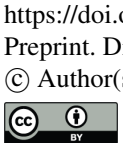

Open Access Earth System Science Data Discussions

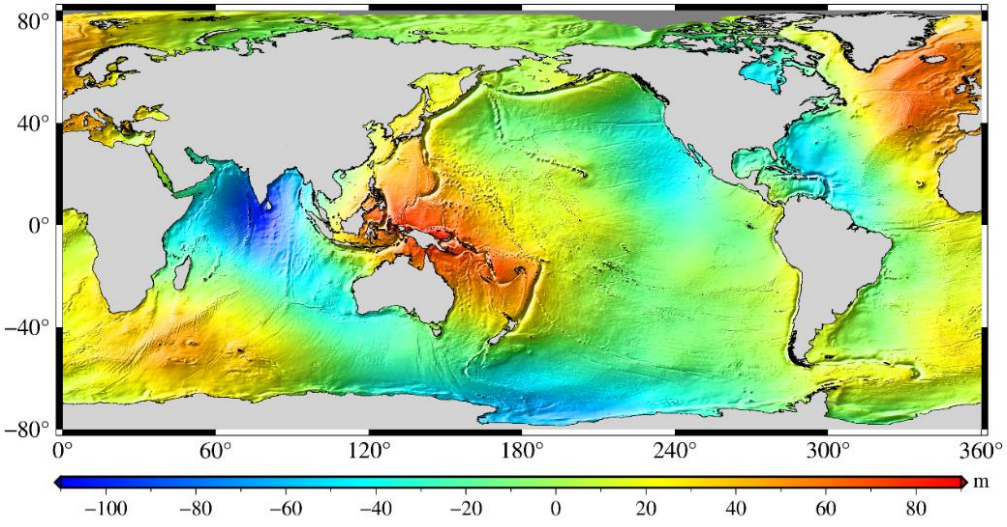

Figure 5. Global mean sea surface model SDUST2020.

4.3 Data availability

The SDUST2020 MSS dataset as .nc file is now available open-access at the site https://doi.org/10.5281/zenodo.6555990 (Yuan et al., 2022). The dataset includes geospatial information (latitude, longitude) and mean sea surface height.

5 Comparison and validation

Here, several independent ways are proposed to validate the SDSUT2020 model. Firstly, inspecting the difference with another MSS models, such as CLS15 and DTU18; secondly, comparing the MSS models with the data of GPS-leveled tide gauges around Japan; finally, comparing with the independent altimeter data including several data of ERM and GM.

5.1 Comparison with CLS15 and DTU18 models

The CLS15 and DTU18 models are current representative MSS models published by different institutions (CLS15 published by CLS and CNES, and DTU18 published by DTU). These two models are used to validate the SDUST2020 model. Table 4 shows the information of SDUST2020, CLS15 and DTU18 models. The main differences between SDSUT2020 and CLS15 and DTU18 are the reference period and the altimeter data ingested. The reference period of SDUST2020 is 1993-2019, while that of CLS15 and DTU18 is 1993-2012. Compared with CLS15 and DTU18, SDSUT2020 ingests more altimeter data. Among these altimeter data, Jason-3, HY-2A and Sentinel-3A (ingested in the SDUST2020 model) are first used to establish an MSS model.

Table 4. Mean sea surface models SDUST2020, CLS15 and DTU18.

MSS model	SDUST2020	CLS15	DTU18
Grid size	1′×1′	1′×1′	1′×1′

https://doi.org/10.5194/essd-2022-178
Preprint. Discussion started: 23 June 2022

Open Access Earth System Science Data Discussions

Reference period		1993–2019	1993–2012	1993–2012
Coverage		80°S–84°N	80°S–84°N	90°S–90°N
Satellite[a]	ERM	T/P, J1, J2, J3, E2, EN, GFO, SA, H2A, S3A	T/P, J1, J2, E2, EN, GFO	T/P, J1, J2, E1, E2, EN, SA
	GM	E1, J1, H2A, SA, C2	E1, J1, C2	J1, C2, SA

[a]Footnote: T/P for Topex/Poseidon, J1 for Jason-1, J2 for Jason-2, J3 for Jason-3, E1 for ERS-1, E2 for ERS-2, EN for Envisat, H2A for HY-2A, C2 for CryoSat-2, S3A for Sentinel-3A, SA for SARAL.

Table 5 shows the comparative statistical results of SDUST2020, CLS15 and DTU18 models in terms of SSH. In the comparison, the ocean variability caused by averaging over distinct periods (27 years from 1993 to 2019 for SDUST2020, and 20 years from 1993 to 2012 for CLS15 and DTU18) have been removed, which are calculated from the monthly averaged grid sea level variation time series between 1993 and 2019 provided by AVISO, with a grid of 15′×15′. Compared with DTU18, STD of SDUST2020 is less than CLS15; compared with CLS15, SDT of SDUST2020 is also less than DTU18; and compared with SDUST2020, STD of CLS15 is less than DTU18. Therefore, it can be inferred that the accuracy of these three models from high to low is SDUST2020, CLS15, DTU18.

Table 5. Statistical results of comparisons between different mean sea surface models (Unit: m).

Model discrepancy	Max	Min	Mean	STD	RMS	Number of points
SDUST2020-CLS15	9.0319	-13.8801	0.0098	0.2083	0.2085	155330402
SDUST2020-DTU18	7.5640	-9.0388	0.0225	0.2775	0.2784	155330402
CLS15-DTU18	13.8590	-7.8108	0.0127	0.2927	0.2930	155330402

If the three models of SDUST2020, CLS15 and DTU18 are not correlated with each other, then according to the error propagation law, the STDs of these three models compared with each other can be expressed as:

$$\begin{cases} STD_{S\_C}{}^2 = STD_S{}^2 + STD_C{}^2 \\ STD_{S\_D}{}^2 = STD_S{}^2 + STD_D{}^2 \\ STD_{C\_D}{}^2 = STD_C{}^2 + STD_D{}^2 \end{cases} \quad (6)$$

where STD_{S_C}, STD_{S_D} and STD_{C_D} are the STD of SDUST2020 compared with CLS15, SDUST2020 compared with DTU18 and CLS15 compared with DTU18, respectively; STD_S, STD_C and STD_D are the STD of SDUST2020, CLS15 and DTU18. According to the statistical results in Table 5, the SDT of SDUST2020, CLS15 and DTU18 can be calculated according to Equation (6), which are about 0.1318 m, 0.1613 m and 0.2442 m, respectively. This result can again confirm that the accuracy of these three models from high to low is SDUST2020, CLS15 and DTU18.

The SSH differences between the SDUST2020, CLS15 and DTU18 models in the long and short wavelengths are shown in Figure 7 (the SSH differences between SDUST2020 and CLS15), Figure 8 (the SSH differences between SDUST2020 and DTU18) and Figure 9 (the SSH differences between CLS15 and DTU18), which are drown after a Gaussian filtering with the tools available in GMT6.0 (Generic Mapping Tools version 6.0) software (Wessel et al., 2019). As the same selected in the

https://doi.org/10.5194/essd-2022-178
Preprint. Discussion started: 23 June 2022

literature Andersen et al. (2018), the wavelength of 150 km is selected as the dividing line of the long and short wavelengths. It can be seen from the Figures 7, 8 and 9 that there are no significant differences between these models in the short wavelength (wavelength less than 150 km), and the average differences are within 2 cm, while there are some significant differences in the long wavelength (wavelength greater than 150 km). The differences between these models in the long wavelength are mainly concentrated in the polar circumpolar region and the western boundary current region (including the Kuroshio Current, Mexico Gulf, Agulhas Current, etc.), and the sea level variation in these regions is relatively large (Jin et al., 2016).

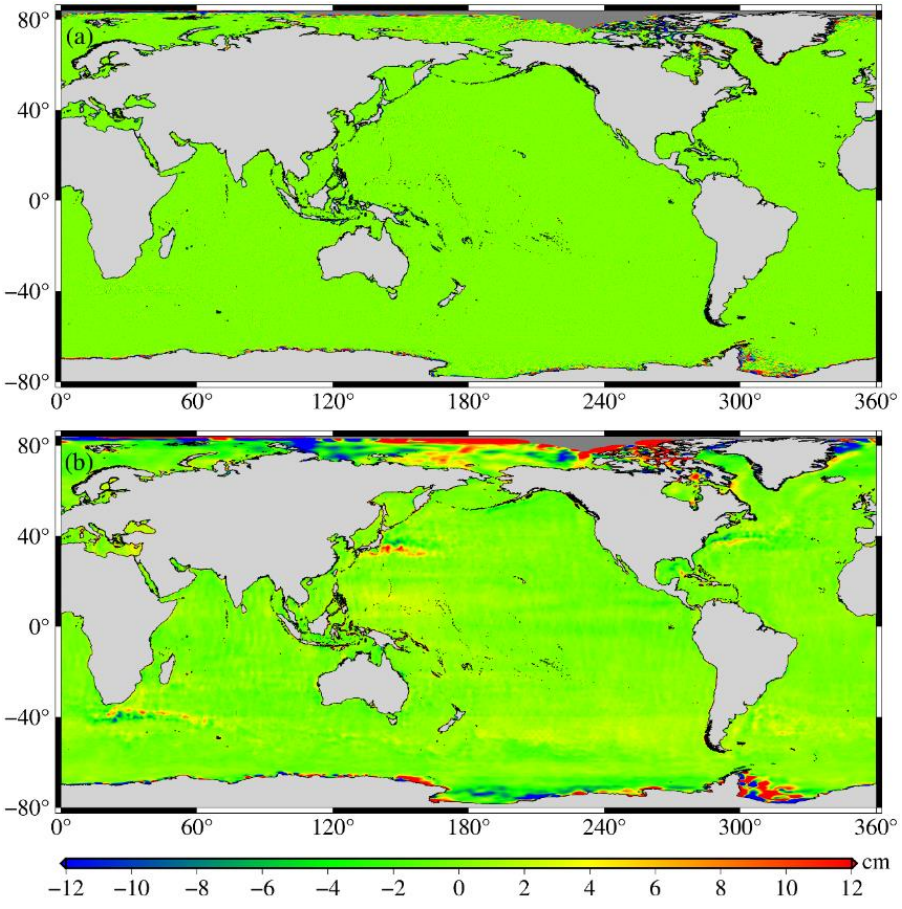

Figure 6. Differences between SDUST2020 and CLS15: (a) where the wavelength is less than 150 km; (b) where the wavelength is greater than 150 km.

https://doi.org/10.5194/essd-2022-178
Preprint. Discussion started: 23 June 2022

Open Access Earth System Science Data Discussions

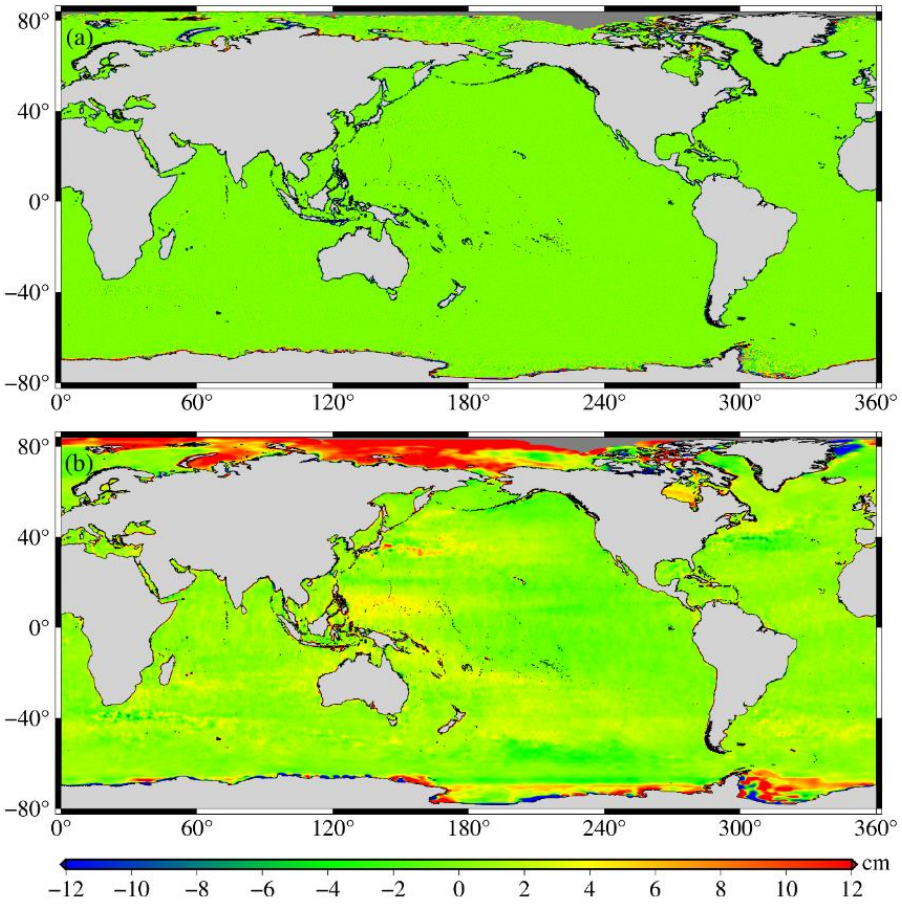

Figure 7. Differences between SDUST2020 and DTU18: (a) where the wavelength is less than 150 km; (b) where the wavelength is greater than 150 km.

https://doi.org/10.5194/essd-2022-178
Preprint. Discussion started: 23 June 2022

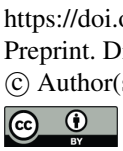

Open Access Earth System Science Data Discussions

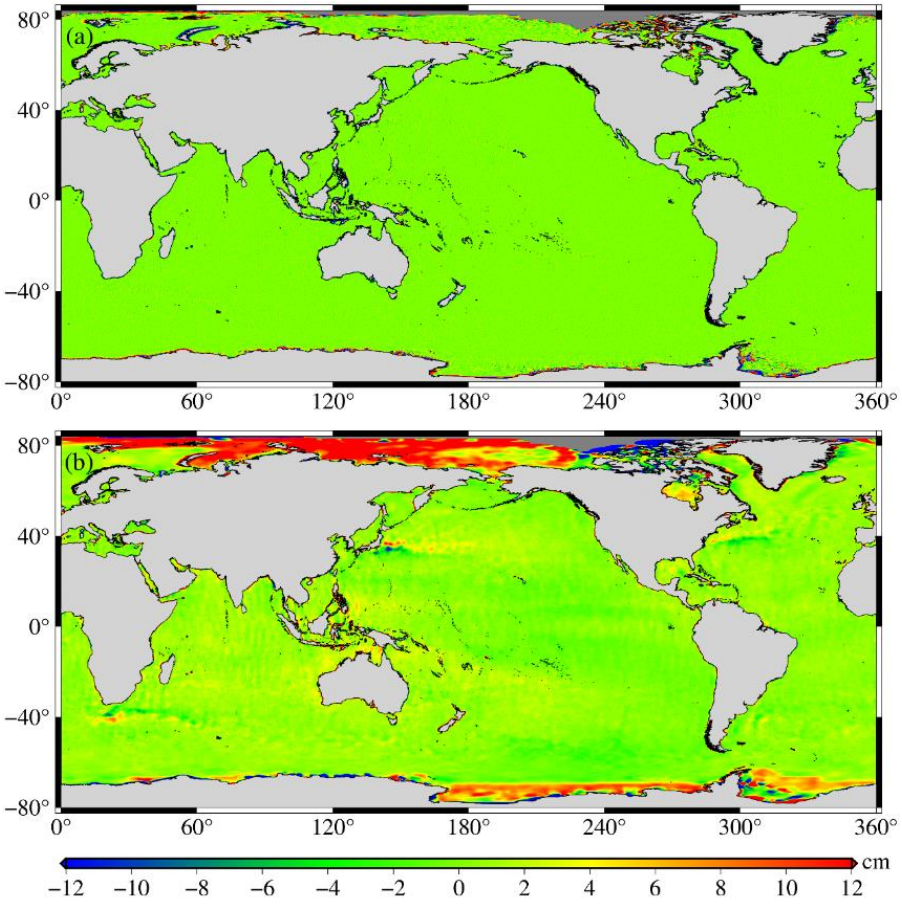

Figure 8. Differences between CLS15 and DTU18: (a) where the wavelength is less than 150 km; (b) where the wavelength is greater than 150 km.

Figures 9, 10 and 11 highlight the formal error of SDUST2020, CLS15 and DTU18, respectively. It can be observed from these figures that the SDUST2020 is much more homogenous and accurate then CLS15 and DTU18. This is also confirmed by the word-wide statistics. The average and RMS about the formal error of SDSUT2020 are 1.0 cm and 1.5 cm, that of CLS15 are1.4 cm and 1.9 cm, and that of DTU18 are1.9 cm and 2.0 cm.

https://doi.org/10.5194/essd-2022-178
Preprint. Discussion started: 23 June 2022

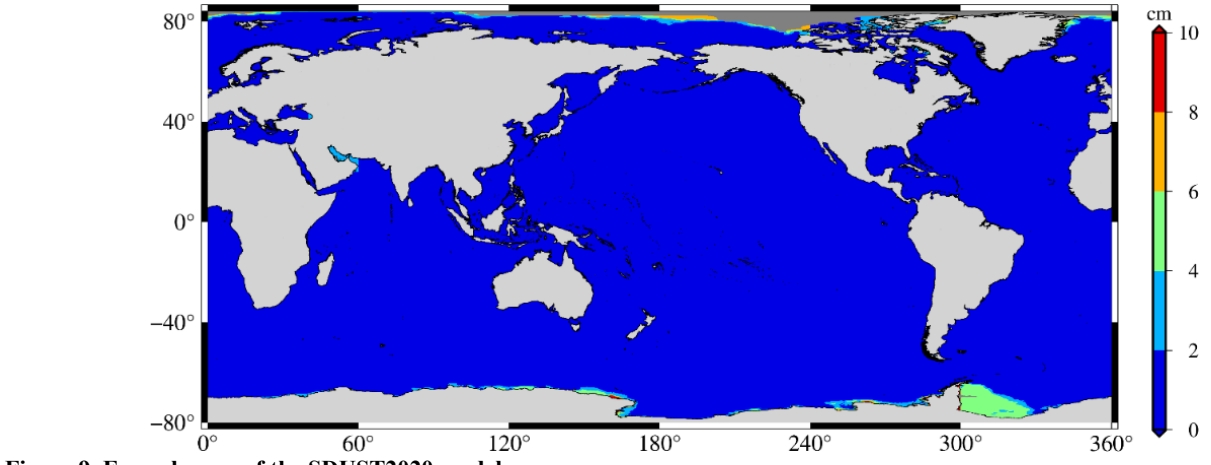

Figure 9. Formal error of the SDUST2020 model.

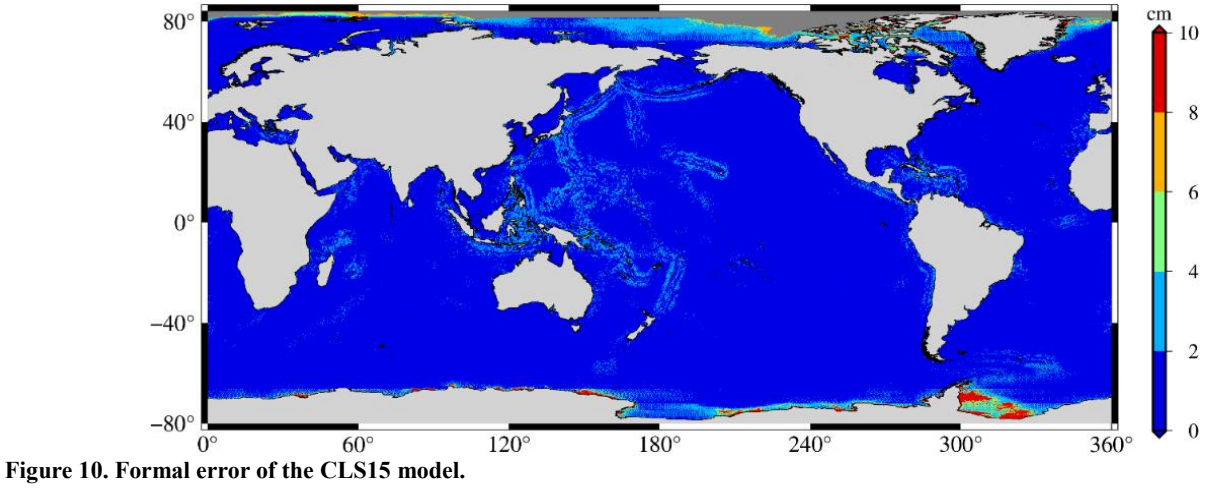

Figure 10. Formal error of the CLS15 model.

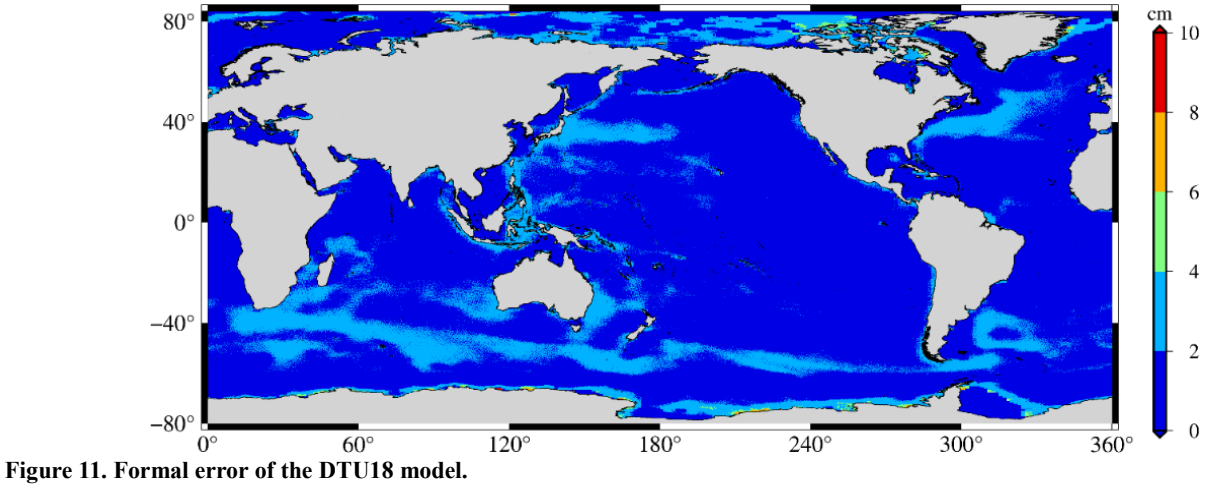

Figure 11. Formal error of the DTU18 model.

https://doi.org/10.5194/essd-2022-178
Preprint. Discussion started: 23 June 2022

5.2 Comparison with GPS-leveled tide gauges

The comparison between a total of 34 GPS-leveled tide gauges around Japan and the SSH of SDUST2020, CLS15 and DTU18 models can independently validate the accuracy differences of these models which are close to the coast (Andersen and Knudsen, 2009). Since it is not clear how wide the SSH can be represented by a single tide gauge. The SSH of different models at the location of tide gauge is calculated by reciprocal weighting of the spherical distance from the tide gauge to the points, these points are determined by different search radii (e.g. 10 km, 20 km, 30 km, 40 km and 50 km) which are centered on the tidal station. The SSH differences of different models compared with 34 GPS-leveled tide gauges around Japan in different search radii are shown in Figure 12, and its STD are shown in Table 6. From Figure 12 and Table 6, it can be observed that the larger the search radii, the greater the difference between the models and the GPS-leveled tide gauges. In Table 6, the STD of SSH differences of SDUST2020 compared with GPS-level tide gauges are smaller than those of CLS15 and DTU18, indicating that the accuracy of SDUST2020 is better than that of CLS15 and DTU18.

Table 6. STD of SDUST2020, CLS15 and DTU18 models compared with GPS-leveled tide gauges around Japan in different search radii (Unit: m)

Search radii	10 km	20 km	30 km	40 km	50 km
SDUST2020	0.1917	0.2102	0.2588	0.3264	0.3911
CLS15	0.2413	0.2296	0.2806	0.3634	0.4385
DTU18	0.2752	0.2777	0.3052	0.3512	0.4003

https://doi.org/10.5194/essd-2022-178
Preprint. Discussion started: 23 June 2022

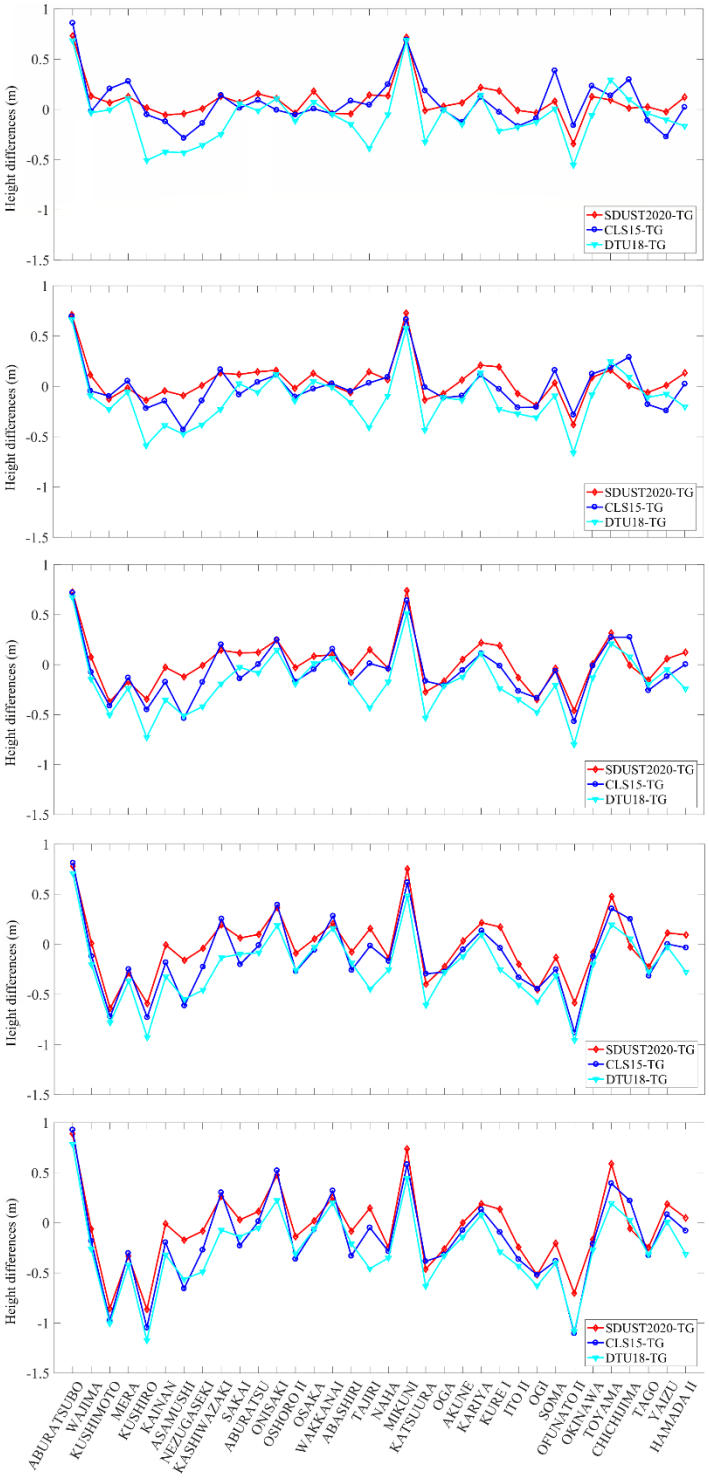

Figure 12. Sea surface height differences of different models compared with 34 GPS-leveled tide gauges around Japan in different search radius. (a), (b), (c), (d) and (e) correspond to the search radius of 10 km, 20 km, 30 km, 40 km and 50 km, respectively.

https://doi.org/10.5194/essd-2022-178
Preprint. Discussion started: 23 June 2022

5.3 Comparison with altimeter data

The comparison with altimeter data can estimates the accuracy of MSS models (Andersen and Knudsen, 2009; Schaeffer et al., 2012; Jin et al., 2016), which is another effective way of validating the MSS models. Several datasets are chosen, including ERM data and GM data. The ERM data are the mean along-track SSH after collinear adjustment, and the GM data are not processed by ocean variability correction. The ERM data include 1-year ERS-1 data, 2-year HY-2A data, 2-year Jason-3 data, 2.5-year Sentinel-3A data and 1-year Sentinel-3B data, and the GM data include 1.5-year Envisat/GM data, 2-month Jason-2/GM data and 1-year HY-2A/GM data. Among these data, the data of Sentinel-3B and Envisat/GM are not ingested in models of SDUST2020, CLS15 and DTU18, and the data of HY-2A, Jason-3 and Sentinel-3A are ingested in the SDUST2020 model, while they are not ingested in models of CLS15 and DTU18.

Table 7 shows the STD of the SSH's differences about the models of SDUST2020, CLS15 and DTU18 compared with altimeter data. From the results in Table 7, the differences between the STD given by these three models are in the millimeter level, but nearly all STDs given by SDSUT2020 are lower than CLS15 and DTU18, which is an indication of higher accuracy. The STDs given by these three models are about 4-6 cm compared with ERM data (the former five groups), and about 10 cm compared with GM data (the last three groups), and the former is almost half of the later. The reason may be that the altimeter data of the former five groups have been corrected for the ocean variability, but those of the last group have been not.

Table 7. STDs of the sea surface height differences of the models SDUST2020, CLS15 and DTU18 compared with satellite altimetry data (Unit: m).

Satellite (period)	SDUST2020	CLS15	DTU18
ERS-1 (1995.04.01–1996.04.30)	0.0529	0.0509	0.0524
HY-2A (2014.04.12–2016.03.15)	0.0565	0.0610	0.0618
Jason-3 (2017.01.01–2018.12.31)	0.0414	0.0431	0.0480
Sentinel-3A (2016.06.28–2018.12.31)	0.0448	0.0479	0.0548
Sentinel-3B (2019.01.01–2019.12.31)	0.0502	0.0522	0.0576
Envisat/GM (2010.10.27–2012.04.08)	0.0999	0.1007	0.1038
Jason-2/GM (2017.07.13–2017.09.13)	0.0991	0.0999	0.1013
HY-2A/GM (2018.12.26–2019.12.30)	0.1180	0.1187	0.1201

To more accurately assess and quantify the differences of model errors about SDUST2020, CLS15 and DTU18 in different wavelengths, the Sentinel-3B data (1-year, 2019.01.01–2019.12.31) are selected to calculate sea level anomaly (SLA) along-track based on these three models and obtain SLA power spectral density (PSD). Since the Sentinel-3B data are independent of these three models, the difference between the SLA PSDs of Sentinel-3B along-track calculated based on these three models reflects the difference in the error of these three models (Pujol et al., 2018; Sun et al., 2021).

https://doi.org/10.5194/essd-2022-178
Preprint. Discussion started: 23 June 2022

Figure 13(a) shows the mean global SLA PSD along Sentinel-3B tracks when different MSS models are used. As show in Figure 13(a), all PSDs vary with the wavelengths, the longer wavelengths the greater PSDs, and there are also differences between PSDs of different MSS models for different wavelengths. Since the SSH and MSS are based on independent data and periods, it can assume that for the long wavelengths (e.g. wavelengths longer than 150 km), the ocean variability signal dominates, for the short wavelengths (e.g. wavelengths from ~25 to 150 km), the errors of MSS models dominate, while for the shorter wavelengths (e.g. wavelengths shorter than 25 km), the altimeter noise floor dominates (Pujol et al., 2018).

The PSD of SDUST2020 model is significantly less than that of CLS15 and DTU18, and the PSD of CLS15 is slightly smaller than that of DTU18 for wavelengths longer than 150 km. The reason of former is that the reference period of SDUST2020 (1993-2019) is longer than that of CLS15 and DTU18 (1993-2012), and the reason of latter is that Sentinel-3B data uses the same data preprocessing as the altimeter data ingested in CLS15 model. This is also confirmed by the world-wide statistics. The average values of the SLA based on SDUST2020, CLS15 and DTU18 are 0.0155 m, 0.0494 m and 0.0596 m, respectively, and the RMS are 0.0525 m, 0.07919 m and 0.0829 m, respectively.

Figure 13(b) shows the ratio between the PSD curves of Figure 13(a), which can better quantify the differences between the MSS models. Compared with the CLS15 model, the errors of SDUST2020 model improve in the wavelength range from 25 to 150 km with a maximal impact around 40 km, which is improved by about 15%.

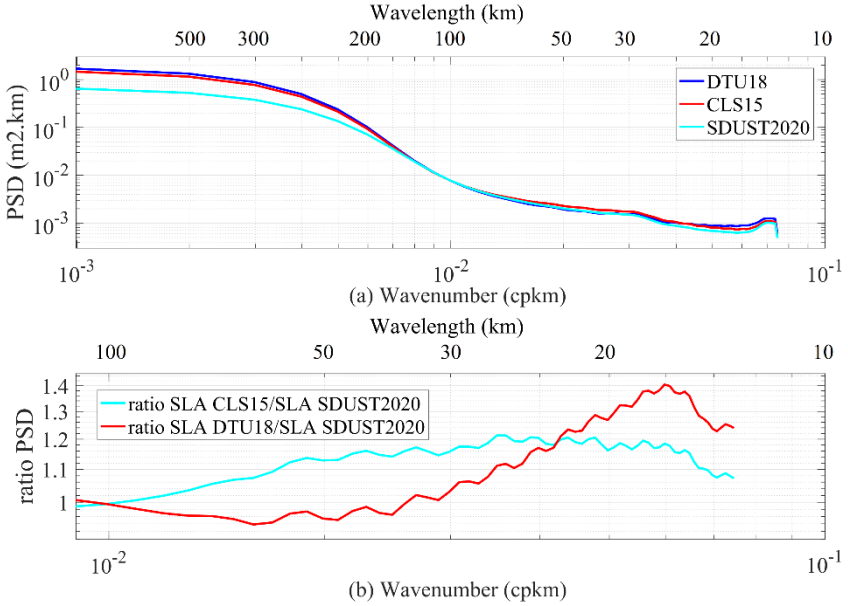

Figure 13. (a) The SLA PSD along Sentinel-3B tracks using several models. (b) The ratio of SLA PSD from panel (a).

https://doi.org/10.5194/essd-2022-178
Preprint. Discussion started: 23 June 2022

Open Access Earth System Science Data Discussions

Table 8 gives the STD about SLA of these three MSS models for wavelengths ranging from 25 to 150 km along different altimeter tracks. The results from Table 8 show that the accuracy difference among these three models is very small, all in the sub-millimeter level, but the accuracy of SDUST2020 is slightly better than that of CLS15 and DTU18.

Table 8. STD of SLA for short wavelengths along the track of different altimeters, based on different MSS models (passband filtered from 25 to 150 km) (Unit: m).

	ERS-1	HY-2A	Jason-3	Sentinel-3A	Sentinel-3B	Envisat/GM	Jason-2/GM	HY-2A/GM
SDUST2020	0.0109	0.0099	0.0073	0.0089	0.0087	0.0201	0.0198	0.0205
CLS15	0.0107	0.0102	0.0067	0.0094	0.0090	0.0201	0.0198	0.0206
DTU18	0.0115	0.0107	0.0076	0.0099	0.0097	0.0202	0.0201	0.0207

6 Conclusions

In this paper, SDUST2020, a new global MSS model is established with 19-year moving average method from multi-satellite altimetry data. Its global coverage is from 80°S to 84°N, grid size is 1'×1', and reference period is from January 1993 to December 2019.

Compared with CLS15 and DTU18 models, first, SDUST2020 model is innovated in the data processing method of model establishment, such as using 19-year moving average method; second, the reference period of the SDUST2020 model extend from 1993 to 2019, while that of CLS15 and DTU18 is from 1993 to 2012; third, the establishment of SDUST2020 model for the first time integrates the altimeter data of HY-2A, Jason-3 and Sentinel-3A which have not been used in the establishment of any other global MSS model.

Comparing SDUST2020 with CLS15 and DTU18 models, the results show that the accuracy of these three models from high to low is SDUST2020, CLS15 and DTU18. Comparing SDUST2020, CLS15 and DTU18 with the data of GPS-leveled tide gauges around Japan and altimeter data of several satellites, all the results show that the accuracy of SDUST2020 is better than that of CLS15 and DTU18.

Appendix A

Table A1. Information of 34 tide gauges stations and joint GPS stations around Japan.

Tide gauge	Longitude (°)	Latitude (°)	GPS station	Height of RLR (m)
ABURATSUBO	139.615278	35.160278	P108	28.874±0.012
WAJIMA	136.900278	37.405833	P111	30.416±0.015
KUSHIMOTO	135.773333	33.475833	P208	31.894±0.008
MERA	139.825000	34.918889	P206	29.398±0.009
KUSHIRO	144.371389	42.975556	P203	22.211±0.007
KAINAN	135.191389	34.144167	P117	31.220±0.007
ASAMUSHI	140.859167	40.897500	P103	30.094±0.009
NEZUGASEKI	139.545833	38.563333	P105	32.528±0.008
KASHIWAZAKI	138.508333	37.356667	P110	32.101±0.009

https://doi.org/10.5194/essd-2022-178
Preprint. Discussion started: 23 June 2022

SAKAI	140.724722	41.781667	P204	27.380±0.009
ABURATSU	131.409444	31.576944	P211	21.404±0.013
ONISAKI	136.823611	34.903889	P116	31.038±0.014
OSHORO II	140.858056	43.209444	P101	25.709±0.013
OSAKA	129.866111	32.735000	P210	25.630±0.014
WAKKANAI	141.685278	45.407778	P201	19.991±0.008
ABASHIRI	144.285833	44.019444	P202	23.227±0.008
TAJIRI	134.315833	35.593611	P118	28.876±0.008
NAHA	127.665278	26.213333	P212	24.530±0.011
MIKUNI	136.148889	36.254722	P112	29.320±0.011
KATSUURA	140.249444	35.129444	P107	26.268±0.009
OGA	139.705833	39.942222	P104	30.603±0.007
AKUNE	130.190833	32.017500	P123	25.594±0.023
KARIYA	129.849167	33.473056	P121	25.069±0.010
KURE I	133.243333	33.333611	P120	29.147±0.010
ITO II	139.133056	34.895556	P113	33.414±0.017
OGI	138.281111	37.814722	P109	31.151±0.008
SOMA	140.962222	37.830833	P106	34.781±0.007
OFUNATO II	141.753333	39.019722	P205	33.347±0.008
OKINAWA	127.824444	26.179444	P124	23.986±0.006
TOYAMA	137.224722	36.762222	P207	31.282±0.008
CHICHIJIMA	142.183333	27.083333	P213	43.154±0.010
TAGO	138.764167	34.806944	P114	33.377±0.009
YAIZU	138.327222	34.870556	P115	33.155±0.009
HAMADA II	132.066111	34.897222	P209	26.624±0.010

Author contributions. All authors have contributed to designing the approach and writing the manuscript.

Competing interests. The contact author has declared that neither they nor their co-authors have any competing interests.

Disclaimer. Publisher's note: Copernicus Publications remains neutral with regard to jurisdictional claims in published maps and institutional affiliations.

Acknowledgments. We are very grateful to AVISO for providing the along-track Level-2+(L2P) products and the delayed-time gridded monthly mean of sea-level anomalies product, which can be obtained by downloading freely from AVISO official website (ftp://ftp-access.aviso.altimetry.fr). We are also thankful to CLS for providing CNES_CLS15 MSS (ftp://ftp-access.aviso.altimetry.fr) and DTU for providing the DTU18 MSS (https://ftp.space.dtu.dk/pub/). The tide gauge records are available online (https://www.psmsl.org/) and the GPS data are available online (https://www.sonel.org).

Financial support. This work was partially supported by the National Natural Science Foundation of China (grants 42192535 and 41774001), the Autonomous and Controllable Project for Surveying and Mapping of China (grant 816517), and the SDUST Research Fund (grant 2014TDJH101).

https://doi.org/10.5194/essd-2022-178
Preprint. Discussion started: 23 June 2022

References

Andersen, O. B., and Knudsen, P.: DNSC08 mean sea surface and mean dynamic topography models, J. Geophys. Res.-Oceans, 114(C11), 327-343, https://doi.org/10.1029/2008JC005179, 2009.

Andersen, O. B., Knudsen, P., Bondo, T.: The mean sea surface DTU10 MSS-comparison with GPS and Tide Gauges, In: ESA Living Planet Symposium, Bergen, 2010.

Andersen, O. B., Knudsen, P., Stenseng, L.: The DTU13 MSS (mean sea surface) and MDT (mean dynamic topography) from 20 years of satellite altimetry, In: Jin, S., Barzaghi, R. (eds) IGFS 2014, International Association of Geodesy Symposia, vol 144, Springer, Cham, https://doi.org/10.1007/1345_2015_182, 2015.

Andersen, O. B., Knudsen, P., and Stenseng, L.: A new DTU18 MSS mean sea surface–improvement from SAR altimetry, In: 25 Years of Progress in Radar Altimetry Symposium, Portugal, 2018.

Andersen, O. B., Vest, A. L., and Knudsen, P.: The KMS04 multi-mission mean sea surface, In: Proceedings of the Workshop GOCINA: Improving Modelling of Ocean Transport and Climate Prediction in the North Atlantic Region Using GOCE Gravimetry, Novotel, Luxembourg, 13-15 April, 2006.

Andersen, O. B., Piccioni, G., Stenseng, L., Knudsen, P.: The DTU15 MSS (mean sea surface) and DTU15LAT (lowest astronomical tide) reference surface, In: Proceedings of the ESA Living Planet Symposium 2016, Prague, 2016.

CNES: Along-track level-2þ (L2P) SLA product handbook. SALPMU-P-EA-23150-CLS, Issue 1.0, https://www.aviso.altimetry.fr/fileadmin/documents/data/tools/hdbk_L2P_all_missions_except_S3.pdf, 2017.

Ducet, N., Le Traon, P. Y., and Reverdin, G.: Global high-resolution mapping of ocean circulation from TOPEX/Poseidon and ERS-1 and -2, J. Geophys. Res.-Oceans, 105(C8), 19477-19498, https://doi.org/10.1029/2000jc900063, 2000.

Guo, J., Hwang, C., and Deng, X.: Editorial: Application of satellite altimetry in marine geodesy and geophysics, Front. Environ. Sci., 10, 910562, https://doi.org/10.3389/feart.2022.910562, 2022.

Holgate, S. J., Matthews, A., Woodworth, P. L., Rickards, L. J., Tamisiea, M. E., Bradshaw, E., Foden, P. R., Gordon, K. M., Jevrejeva, S., and Pugh, J.: New Data Systems and Products at the Permanent Service for Mean Sea Level, J. Coastal Res., 29(3), 493-504, https://doi.org/10.2112/JCOASTRES-D-12-00175.1, 2013.

Huang, M., Zhai, G., Ouyang, Y., Lu, X., Liu, C., and Wang, R.: Integrated data processing for multi-satellite missions and recovery of marine gravity field, Terr. Atmos. Ocean. Sci., 19, 103-109, https://doi.org/10.3319/TAO.2008.19.1-2.103(SA), 2008.

Hwang, C.W.: High precision gravity anomaly and sea surface height estimation from Geos-3/Seasat altimeter data, M.S. Thesis. Dept. of Geodetic Science and Surveying, The Ohio State University, Columbus, OH, USA, 1989.

Jin, T., Li, J., Jiang, W: The global mean sea surface model WHU2013, Geod. Geodyn., 7, 202-209, http://dx.doi.org/10.1016/j.geog.2016.04.006, 2016.

Jordan, S. K.: Self-consistent statistical models for the gravity anomaly, vertical deflections, and undulation of the geoid, J. Geophys. Res., 77(20), 3660–3670, https://doi.org/10.1029/JB077i020p03660, 1972.

https://doi.org/10.5194/essd-2022-178
Preprint. Discussion started: 23 June 2022

Le Traon, P. Y., Dibarboure, G., and Ducet, N.: Use of a high-resolution model to analyze the mapping capabilities of multiple-altimeter missions, J. Atmos. Ocean. Tech., 18(7), 1277-1288, https://doi.org/10.1175/1520-0426(2001)018<1277:UOAHRM>2.0.CO;2, 2001.

Le Traon, P. Y., Faugère, Y., Hernandez, F., Dorandeu, J., Mertz, F., and Ablain, M.: Can we merge GEOSAT follow-on with TOPEX/Poseidon and ERS-2 for an improved description of the ocean circulation?, J. Atmos. Ocean. Tech., 20(6), 889-895, https://doi.org/10.1175/1520-0426(2003)020<0889:CWMGFW>2.0.CO;2, 2003.

Le Traon, P. Y., Nadal, F., and Ducet, N.: An improved mapping method of multisatellite altimeter data, J. Atmos. Ocean. Tech., 15(2), 522-534, https://doi.org/10.1175/1520-0426(1998)015<0522:AIMMOM>2.0.CO;2, 1998.

Moritz, H.: Least-squares collocation, Rev. Geophys., 16(3), 421–430, https://doi.org/10.1029/RG016i003p00421, 1978.

Pujol, M.-I., Schaeffer, P., Faugère, Y., Raynal, M., Dibarboure, G., and Picot, N.: Gauging the improvement of recent mean sea surface models: a new approach for identifying and quantifying their errors, J. Geophys. Res.-Oceans, 123(8), 5889-5911, https://doi.org/10.1029/2017JC013503, 2018.

Rapp, R. H., and Bašić, T.: Oceanwide gravity anomalies from GEOS-3, Seasat and Geosat altimeter data, Geophys. Res. Lett., 19(19), 1979-1982. https://doi.org/10.1029/92GL02247, 1992.

Santamaria-Gomez A., Gravelle M., Dangendorf S., Marcos, M., Spada, G., and Wöppelmann, G.: Uncertainty of the 20th century sea-level rise due to vertical land motion errors, Earth. Planet. Sc. Lett., 473, 24-32, https://doi.org/10.1016/j.epsl.2017.05.038, 2017.

Schaeffer, P., Faugére, Y., Legeais, J. F., Ollivier, A., Guinle, T., and Picot, N.: The CNES_CLS11 global mean sea surface computed from 16 Years of satellite altimeter data, Mar. Geod., 35, 3-19, https://doi.org/10.1080/01490419.2012.718231, 2012.

Sun, W., Zhou, X., Yang, L., Zhou, D., and Li, F.: Construction of the mean sea surface model combined HY-2A with DTU18 MSS in the antarctic ocean, Front. Environ. Sci., 9, 697111, https://doi.org/10.3389/fenvs.2021.697111, 2021.

Wessel, P., Luis, J. F., Uieda, L., Scharroo, R., Wobbe, F., Smith, W. H. F., and Tian, D.: The generic mapping tools version 6, Geochem. Geophy. Geosy., 20(11), 5556-5564, https://doi.org/10.1029/2019GC008515, 2019.

Yuan, J., Guo, J., Liu, X., Zhu, C., Niu, Y., Li, Z., Ji, B., and Ouyang, Y.: Mean sea surface model over China seas and its adjacent ocean established with the 19-year moving average method from multi-satellite altimeter data, Cont. Shelf Res., 192(1), 104009, https://doi.org/10.1016/j.csr.2019.104009, 2020.

Yuan, J., Guo, J., Zhu, C., Hwang, C., Yu, D., Sun, M., and Mu, D.: High-resolution sea level change around China seas revealed through multi-satellite altimeter data, Int. J. Appl. Earth Obs., 102, 102433, https://doi.org/10.1016/j.jag.2021.102433, 2021.

Yuan, J., Guo, J., Zhu, C., Li, Z., Liu, X., and Gao, J.: SDUST2020 MSS: A global 1′×1′ mean sea surface model determined from multi-satellite altimetry data [Data set], https://doi.org/10.5281/zenodo.6555990, 2022.